Assembly of SBA-15 into hierarchical porous monoliths replicating polymeric scaffolds

Rıdvan Yildiz, Yannick Lorgouilloux, Jérémy Dhainaut, Carmen Ciotonea, Jean-Philippe Dacquin, Sébastien Royer, Christian Courtois

▶ **To cite this version:**

Rıdvan Yildiz, Yannick Lorgouilloux, Jérémy Dhainaut, Carmen Ciotonea, Jean-Philippe Dacquin, et al.. Assembly of SBA-15 into hierarchical porous monoliths replicating polymeric scaffolds. Microporous and Mesoporous Materials, 2022, 337, pp.111908. 10.1016/j.micromeso.2022.111908 . hal-03644995

HAL Id: hal-03644995
https://hal.univ-lille.fr/hal-03644995v1

Submitted on 19 Apr 2022

HAL is a multi-disciplinary open access archive for the deposit and dissemination of scientific research documents, whether they are published or not. The documents may come from teaching and research institutions in France or abroad, or from public or private research centers.

L'archive ouverte pluridisciplinaire **HAL**, est destinée au dépôt et à la diffusion de documents scientifiques de niveau recherche, publiés ou non, émanant des établissements d'enseignement et de recherche français ou étrangers, des laboratoires publics ou privés.

Journal Pre-proof

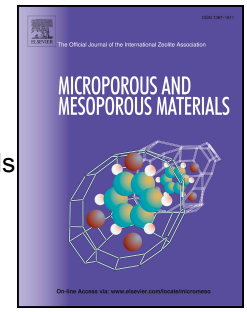

Assembly of SBA-15 into hierarchical porous monoliths replicating polymeric scaffolds

Ridvan Yildiz, Yannick Lorgouilloux, Jérémy Dhainaut, Carmen Ciotonea, Jean-Philippe Dacquin, Sébastien Royer, Christian Courtois

PII: S1387-1811(22)00226-8

DOI: https://doi.org/10.1016/j.micromeso.2022.111908

Reference: MICMAT 111908

To appear in: *Microporous and Mesoporous Materials*

Received Date: 22 December 2021

Revised Date: 21 March 2022

Accepted Date: 5 April 2022

Please cite this article as: R. Yildiz, Y. Lorgouilloux, Jéé. Dhainaut, C. Ciotonea, J.-P. Dacquin, Sé. Royer, C. Courtois, Assembly of SBA-15 into hierarchical porous monoliths replicating polymeric scaffolds, *Microporous and Mesoporous Materials* (2022), doi: https://doi.org/10.1016/j.micromeso.2022.111908.

This is a PDF file of an article that has undergone enhancements after acceptance, such as the addition of a cover page and metadata, and formatting for readability, but it is not yet the definitive version of record. This version will undergo additional copyediting, typesetting and review before it is published in its final form, but we are providing this version to give early visibility of the article. Please note that, during the production process, errors may be discovered which could affect the content, and all legal disclaimers that apply to the journal pertain.

© 2022 Published by Elsevier Inc.

Graphical Abstract

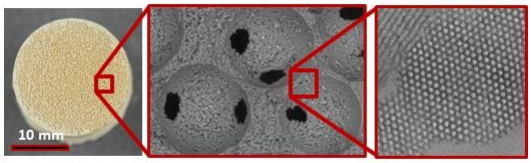

Journal Pre-proof

Journal Pre-proof

Assembly of SBA-15 into hierarchical porous monoliths replicating polymeric scaffolds

Ridvan Yildiz[a,b], Yannick Lorgouilloux[a], Jérémy Dhainaut[b]*, Carmen Ciotonea[b], Jean-Philippe Dacquin[b], Sébastien Royer[b], Christian Courtois[a]*

[a] Univ. Polytechnique Hauts-de-France, CERAMATHS - Laboratoire de Matériaux Céramiques et de Mathématiques, Département Matériaux et Procédés, F-59313 Valenciennes, France

[b] Univ. Lille, CNRS, Centrale Lille, Univ. Artois, UMR 8181 - UCCS - Unité de Catalyse et Chimie du Solide, F-59000 Lille, France

*Corresponding Authors: yannick.lorgouilloux@uphf.fr ; jeremy.dhainaut@univ-lille.fr

Journal Pre-proof

Journal Pre-proof

Abstract:

This study reports the preparation of highly porous, SBA-15-based monolithic materials with pore sizes spanning over four scales (micro-/meso-/small macro-/large macro-pores). Two approaches were explored. The first one involves the preparation of PMMA scaffolds obtained from chemically-bonded beads and their further infiltration using SBA-15 slurries with suitable viscosity; while the second one directly uses the same amount of PMMA beads dispersed within the slurries. Emphasis was given to the comparison of the textural, structural, and mechanical properties obtained following each approach. Then, application of a thermal consolidation step and its influence over the monoliths properties was investigated, with an optimum observed at 950 °C. The second method systematically allowed reaching higher mechanical resistances (86 vs 32 kPa at 950 °C) for comparable specific surface areas (274 vs 290 m^2/g at 950 °C), however at the expense of smaller macropores and lower ordering in the monoliths.

Keywords: SBA-15; hierarchical porous materials; monoliths; shaping technique; slurry infiltration

Journal Pre-proof

Journal Pre-proof

1. Introduction

Hierarchical porous structures can be found in various natural materials including leaves, bones, and wood. While being light cellular structures, their specific hierarchical arrangement ensures high strength and flexibility [1]. Besides, hierarchical porous materials have been increasingly studied over the past decade as they present several advantages compared to single-sized porous materials. Being constituted of pores spanning over several scales, each scale solves the drawback of another one: micropores and small mesopores provide high surface area and molecular sieving ability, but they present significant diffusion restrictions; while macropores minimize diffusion barriers and enhance the accessibility to active sites, yet their contribution to the total surface area is low. Therefore, these materials typically present superior performances in separation, energy, life science and heterogeneous catalysis [2].

SBA-15 is an ordered mesoporous silica that has been widely applied to heterogeneous catalysis, as a catalyst support [3]. Its framework is composed of cylindrical mesopores with calibrated diameters from 5 to 10 nm, arranged hexagonally following the space group P6mm, and providing a surface area reaching up to 1000 m^2/g [4]. Interestingly, SBA-15 presents higher thermal and hydrothermal stability than other porous silicas, including the M-41S family, owing to its thick pore walls. In addition, its hexagonal pores are interconnected through irregular micropores: SBA-15 is thus considered a bi-modal micro-/mesoporous material [5], a unique characteristic that can be advantageously used to stabilize active nanoparticles in a divided state [6][7]. Still, consequent diffusional restrictions appear when the catalytic conversion of bulky molecules is required, limiting the catalytic activity [8]. These restrictions can be lifted by introducing macropores.

Hierarchical, meso-/macroporous silica-based materials can be obtained following various ways including inverse opals [8], freeze-casting [9], additive fabrication [10], spinodal decomposition (also known as phase separation) [11], and foaming [12]. The resulting materials are usually macrostructured, meaning that they present a controlled geometry replicating the shape of the receptacle in which they were prepared. Moreover, depending on the technique used, a large choice of macrostructures and macroporous networks can be achieved: from straight (freeze-casting, additive fabrication) to tortuous (inverse opals, spinodal decomposition) macropores, and with (inverse opals) or without (additive

fabrication, freeze-casting) interconnections. The size and the morphology of the macropores can also be directed to some extent.

By carefully controlling these parameters, the thermal conductivity and mass transfer can be tuned, with a direct impact over the final performances of the materials. Moreover, the ability to fine-tune the macroporous network allows multiscale flow modelling, and therefore an improved comprehension of the catalyzed reaction processes. Hence, it is of significant importance to develop new techniques to improve this control. In this line, we developed an approach based on the replication of a polymer scaffold made from partially fused beads, leading to controlled interconnectivity [13]. While this approach was developed for bone regeneration applications starting from hydroxyapatite [14], it is worth investigating its use for the preparation of hierarchical porous materials made from an organized mesoporous silica, for applications as catalyst supports.

Hence, SBA-15-based hierarchical monoliths were prepared starting from polymer scaffolds and SBA-15 slurries with appropriate viscosity. The resulting materials were extensively characterized and compared to classical hierarchical monoliths prepared by inverse opals, where the polymer beads were simply mixed with the slurry and left to sediment. Such hierarchical monoliths are promising materials for continuous flow microreactors [15], however the consequent pressure drop applied in these conditions require the use of mechanically-resistant materials. To meet this challenge, emphasis was given to improving the crushing strength of the as-prepared monoliths following thermal treatments.

2. Experimental

2.1. Materials preparation

Hydrochloric acid (HCl, 37 wt.%), tetraethyl orthosilicate (TEOS), Pluronic EO_{20}-PO_{70}-EO_{20} (P123), and poly(methyl methacrylate) (PMMA) beads were purchased from VWR, Aldrich, Sigma-Aldrich, and Diakon Ineos Acrylics, respectively. All reactants were used as-received. After sieving, only the PMMA beads granulometric fraction between 300 and 400 μm was used (see Figure S1).

2.1.a. Preparation of SBA-15 slurries

SBA-15 was prepared according to the literature [3]. More details are given in SI.

Aqueous slurries were prepared with a concentration of 10 wt.% SBA-15 unless stated otherwise. To ensure stability of the green bodies (objects after assembly and before thermal treatment) during the debinding step, an anionic acrylic latex binder (Duramax B1001, Dow Chemical Company) was added (4 wt.% of SBA-15 weight), based on previous optimizations [15]. This compound is stable up to 220 °C, and its combustion is complete from 500 °C as seen on Figure S2. The slurries were mixed in a planetary ball mill using containers and balls (diameter = 0.5 cm) in agate for 2 hours prior to their use.

2.1.b. Preparation of SBA-15 monoliths: infiltration approach

In a first step, cylindrical scaffolds of PMMA beads were prepared [14]. One gram of beads were placed in a die of inner diameter 16 mm. Acetone was then delicately poured over the PMMA beads, causing their superficial dissolution and partial merging at their contact points. Once the desired shrinkage was reached, the polymeric scaffold was recovered, immerged into distilled water to stop the reaction, and then dried at room temperature overnight.

For infiltrating the PMMA scaffolds, a PVC cylinder with 16-mm machined holes was placed over a Büchner funnel and a filter, and sealed with silicone to apply vacuum through the occupied holes only. After placing the PMMA scaffold in a hole and applying vacuum, the SBA-15 slurry was slowly poured over until complete coverage. Vacuum was maintained 30 minutes, before recovery of the monoliths which were left to dry at room temperature overnight.

2.1.c. Preparation of SBA-15 monoliths: dispersion approach

The same PVC cylinder was placed on a plaster board, and one gram of PMMA beads were placed in each 16-mm hole. SBA-15 slurries were poured over the beads with a pipette while manually stirring, until an adequate volume was filled. The resulting solids were recovered after being fully dried.

2.1.d. Thermal treatments

A debinding treatment was carried out to eliminate the PMMA. A first plateau of 30 hours at 220 °C (heating rate 1°C/min) allows melted PMMA to flow out of the monoliths, while the second and third

dwells of 5 hours each, at 250 °C and 300 °C respectively (heating rate 1 °C/min), allow the combustion of the residual organic matter.

For mechanical reinforcement, the SBA-15 monoliths were further thermally treated under air at temperatures between 550°C and 1100°C in a muffle furnace. Unless stated otherwise, the applied temperature ramp was 1.5°C/min, and a plateau of 3 hours was applied when the targeted temperature was reached.

2.2. Characterization

Nitrogen sorption measurements were performed at 77 K on a Micromeritics Tristar II Plus. Samples were outgassed at 473 K during 6 h before analysis. Specific surface areas (S_{BET}) were calculated according to the Brunauer-Emmet-Teller (BET) method. Total pore volumes (V_{pore}) were measured at P/P_0 = 0,99 from the desorption branch. Average pore diameters (d_{pore}) were determined by the Barrett-Joyner-Halenda (BJH) equation applied to the desorption branch. The viscosity of slurries was measured at 20 °C on a Bohlin Gemini 200 equipped with a 2 °/55 mm cone. Compressive mechanical tests were carried out with a Testometric M250-3CT equipped with a force sensor of 10 kgf. The cylindrical monoliths were placed between two anvils and the load was applied along the axis of the samples until failure. Small angle X-ray Scattering (SAXS) experiments were performed at room temperature on a Xeuss 2.0 (Xenocs) operating under vacuum with a GeniX3D microsource (λ = 1.54 Å) at 0.6 mA and 50 kV and a 2D Pilatus 3R 200K detector. The sample-to-detector distance was 1005 mm. Mercury porosimetry was carried out on a Micromeritics Autopore IV 9500 using a 5 cm^3 penetrometer. Scanning electron microscopy (SEM) observations were done on a Hitachi SU5000 (BSE 15 kV). The open porosity of the PMMA scaffolds was determined following the Archimedes' method (hydrostatic weighing) in deionized water at room temperature. Thermogravimetrical analysis (TGA) under air flow was made using a Setaram Labsys Evo analyzer.

3. Results and discussion

3.1. Preparation of hierarchical porous monoliths

As for any process based on slurry infiltration, the properties of the slurry are crucial to obtain a proper replication of the infiltrated structures. In particular, to allow fast replication of the scaffolds, the dry matter should be as high as possible. However, high solids content might also lead to a considerable increase of the viscosity of the slurry. Therefore, a compromise is required. In the literature, SBA-15 slurries with up to 24 wt.% loading were prepared, however for the washcoating of a iron/chromium alloy [16]. This application requires slurries with significantly higher viscosities than needed for infiltration. Thus, different slurries with a varying amount of SBA-15, from 5 wt.% to 20 wt.%, were prepared and mixed for 2 hours in a planetary ball mill. As related by Perez *et al.* [16], stirring allows breaking SBA-15 agglomerates and dispersing the individual SBA-15 grains, resulting in a lower measured viscosity. Figure 1 presents the dynamic viscosity of the prepared slurries, measured at room temperature. From 5 wt.% to 18 wt.% of SBA-15, a similar shear-thinning behaviour is observed and the instant viscosity increases slightly with the dry matter content. On the other hand, starting from 19 wt.% a shear-thickening behaviour, along with considerably higher instant viscosities, can be observed.

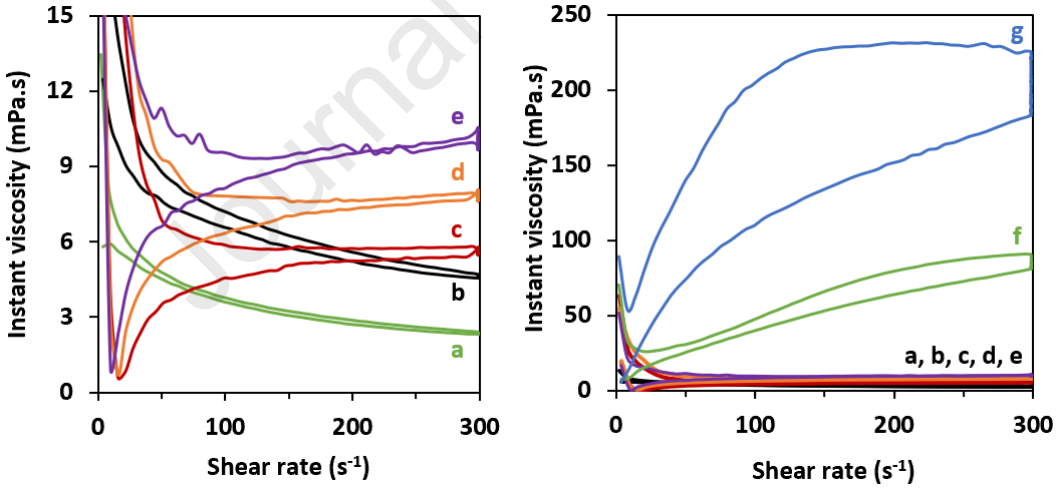

Figure 1: Instant viscosity of SBA-15 slurries in relation to their dry matter content and the applied shear rate: (a) 5 wt.%, (b) 10 wt.%, (c) 15 wt.%, (d) 17 wt.%, (e) 18 wt.% and (f) 19 wt.%, (g) 20 wt.%.

As planetary ball milling is energetic and thus might affect the properties of the material, a 10 wt.% SBA-15 slurry was dried and the resulting powder was compared to the initial SBA-15 powder. The agglomerates were effectively broken into individual SBA-15 grains during ball milling as observed in

Figure 2. More intriguingly, a slight abrasion occurs on the external surface of the grains, which became less rounded. However, the mesoporous structure of SBA-15 was preserved, as similar isotherms of Type IV with H1 hystereses can be observed in Figure 2.e relating to nitrogen physisorption measurements. As further indicated in Table S1, the slurry preparation only accounts for a 8 % decrease of the initial textural properties (S_{BET} lowered from 833 m^2/g to 770 m^2/g). Of note, 4 % of this decrease is due to the presence of the binder, B1001. In comparison, after 24 hours of magnetic stirring Perez *et al.* reported a loss of 25 % of the initial surface area [16]. Therefore, the slurry preparation protocol applied in this study is suitable for SBA-15 phase.

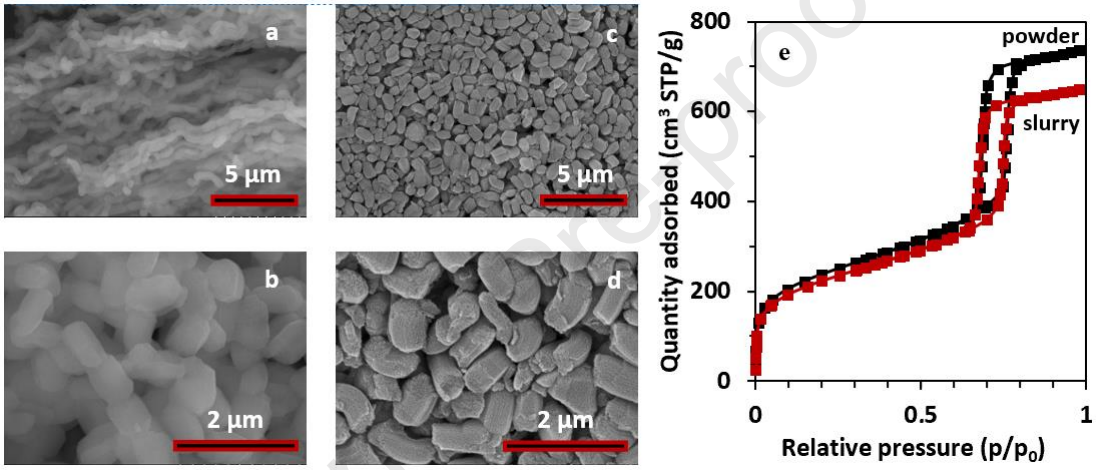

Figure 2: SEM micrographs of (a, b) SBA-15 powder, (c, d) dried SBA-15 slurry and (e) nitrogen physisorption isotherms of SBA-15 powder and dried SBA-15 slurry.

Before use, the PMMA scaffolds (Figure 3, insert) were also characterized. SEM observations reveal that the PMMA beads adopted a close packing and are partially merged with up to six other beads through 80 to 120 µm boundaries. After replication, interconnection windows of similar sizes should be obtained. From mercury porosimetry, displayed in Figure S3, the macropore size distribution in PMMA scaffolds is centered around 100 µm. This is almost two orders of magnitude above the size of the SBA-15 grains as observed in Figure 2: thus, a good replication of the macrostructure is expected. Moreover, hydrostatic weighing measurements were conducted over three scaffolds and summarized in Table S2. The mean percentage of open porosity is comprised between 37.4 and 39.5 %, corresponding to a close stacking.

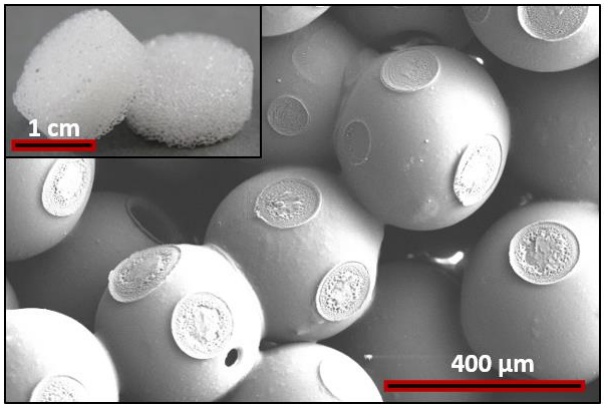

Figure 3: SEM micrographs of polymeric scaffolds of PMMA prepared with 300-400 µm beads. (Insert: Photograph of sacrificial scaffolds of PMMA beads).

The SBA-15 slurries were then used for the infiltration of PMMA scaffolds, and the resulting solids are presented in Figure S4. Slurries with 19 wt.% SBA-15 or above were paste-like and resulted in a poor replication of the scaffolds, as most of the SBA-15 remained above the scaffolds. Below 19 wt.% of SBA-15, all slurries resulted in the formation of macroporous monoliths. Especially, homogeneous monoliths were obtained with a slurry containing 10 wt.% of SBA-15. Thus, this formulation was used for the rest of the study.

Hierarchical porous monoliths were prepared following both the infiltration and the dispersion methods, and photographs and SEM micrographs of the relating debinded materials can be observed in Figure 4. At the macroscale, the SBA-15 monoliths are homogeneous and completely macroporous. However, significant differences appear when making observations at the macropore scale. As expected, the monoliths prepared following the dispersion method show a less compact arrangement of macropores than following the infiltration method as the PMMA beads are not pre-arranged and partially merged. As a result, thicker walls are obtained using the dispersion approach, which could improve the mechanical resistance of the object. Also, the macropore interconnection windows are smaller (around 50 µm for the dispersion approach vs. 80 µm for the infiltration approach) and they are fewer when using the dispersion method, as anticipated. Indeed, the beads are in single contact point configuration after sedimentation. This thus underlines the advantage of the infiltration method for applications where fast inner diffusion is required.

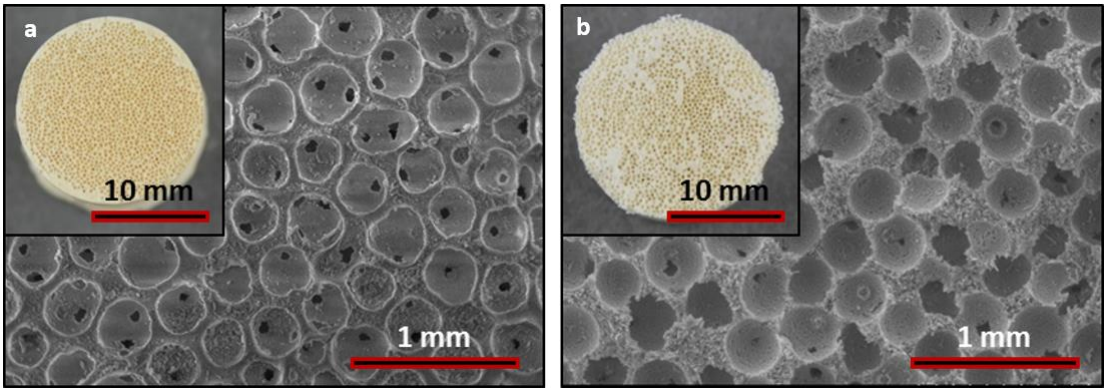

Figure 4: SEM micrographs of debinded hierarchical porous monoliths prepared following (a) the infiltration method, and (b) the dispersion method. Insert: corresponding photographs.

Table 1 lists the textural and structural properties of both types of hierarchical porous monoliths. Importantly, the method does not impact much the physical properties of the SBA-15 grains. Both materials present specific surface areas slightly lower (-11 to -13 %) than the SBA-15 powder recovered from the slurry, which may be explained by the presence of residual organic compounds derived from PMMA elimination within the porosity of the SBA-15. Indeed, as observed in Figure 4, the monoliths are slightly yellow while SBA-15 is white. Moreover, both the hystereses (Figure S5) and the low-angle diffraction peaks (Figure S6) remain unshifted as compared to the powder. Especially, the main peak indexed to (100) plane and the two weak peaks corresponding to (110) and (200) planes are the fingerprints of a P6mm hexagonal pore arrangement. Hence, the pore structure of SBA-15 is retained after debinding.

Table 1: Textural and structural properties of the SBA-15 powder recovered from the slurry (SBA15-slur) and hierarchical porous monoliths after debinding prepared following the infiltration (Mono-Infil) and dispersion (Mono-Disp) methods.

Sample	N_2 physisorption S_{BET} (m^2/g)	N_2 physisorption V_{pores} (cm^3/g)	d_{meso} (nm)	PXRD a_0 (nm)	Hg intrusion d_{pores} (µm)	Bulk density (cm^3/g)
SBA15-slur	770	1.00	6.5	11.5	-	-
Mono-Infil	670	0.97	6.8	11.5	69.1	1.33
Mono-Disp	684	0.98	6.6	11.5	49.7	1.18

Mercury intrusion porosimetry shows that macropore interconnection windows are indeed smaller with the dispersion method than the infiltration method (Figure 5). The size distribution of these windows is also slightly narrower for the infiltration method compared to the dispersion method. Interestingly,

monoliths prepared with the dispersion method present higher macropore volumes (20% more) that those prepared with the infiltration method. Since the infiltration method uses a vacuum pump, it could lead to a high compaction level of the SBA-15 grains. At the opposite, the dispersion method is based on the sedimentation of the slurry, hence generating a looser compaction of the SBA-15 powder. This is further attested by the higher bulk density of the debinded monoliths obtained by infiltration (1.33 cm^3/g) against those obtained by dispersion (1.18 cm^3/g).

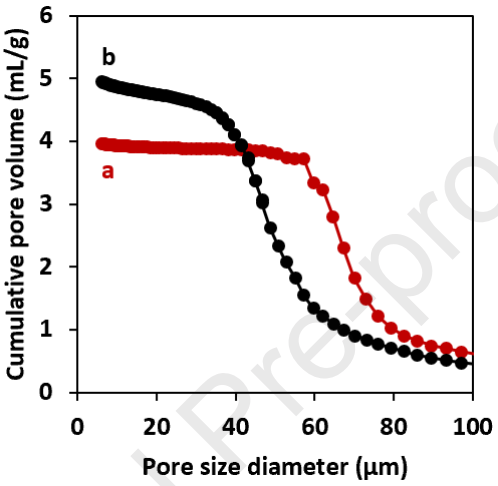

Figure 5: Mercury intrusion porosimetry of SBA-15 monoliths prepared with (a) the infiltration method and (b) the dispersion method. All samples were treated at 550°C.

While the debinded monoliths present a well-defined hierarchical porosity as assessed by N_2 sorption, XRD and SEM, which is appropriate for applications including heterogenous catalyst supports, their mechanical stability needs to be determined. Indeed, strong constraints are typically applied on the catalyst bodies during applications under continuous flow including convection phenomena, attrition in-between the bodies, and pressure drop. Furthermore, generation of fine particles might endanger the whole process by increasing the internal pressure, as well as reducing the overtime performances of the solids. Hence, mechanically-resistant monoliths are critical in consideration of their potential applications.

Figure 6 presents representative stress-strain curves of debinded monoliths prepared following the infiltration and the dispersion methods. The monoliths behave like “elastic-brittle foams” [17] as their compressive stress-strain curves show three distinct kinds of regime: linear elasticity (I), collapse by brittle crushing of the macropores, where stress is almost constant (II), and a densification due to the

compaction of debris formed during the crushing step, where stress drastically increases (III). For the monoliths obtained following the infiltration method, the maximum stress applied at the end of the elastic region (where the monoliths fail and fracture), also called crushing strength, is 13 kPa. As expected from SEM analysis, and while the bulk density of the infiltrated monoliths is higher, the monoliths prepared following the dispersion method have a slightly higher crushing strength (17 kPa) owing to their thicker macropore walls. It remains nonetheless fairly low. Therefore, mechanical reinforcement of the monoliths is required.

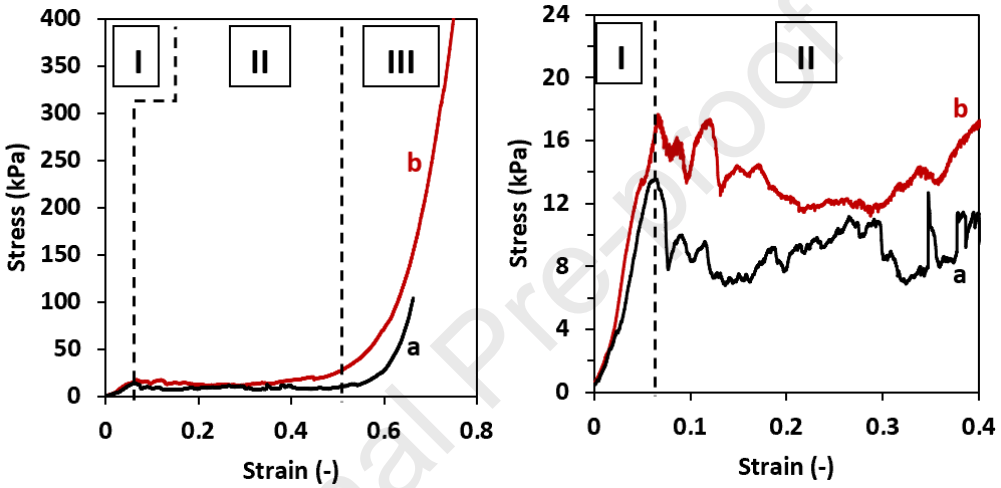

Figure 6: Stress-strain curves showing the mechanical behavior of debinded SBA-15 monoliths prepared from a slurry of 10 wt.% SBA-15 following (a) the infiltration method and (b) the dispersion method. Three regimes are visible: I) linear elastic region, II) brittle crushing and III) densification.

Journal Pre-proof

3.2. Mechanical reinforcement of the monoliths through partial sintering

There is a direct correlation between the density of the materials – and hence their total porosity – and their mechanical resistance [18]. Herein, the hierarchical porous monoliths present a total porosity of about 92 %. Thus, lowering the porosity in a controlled fashion, through partial sintering of the SBA-15 grains, should result in a significant increase of the measured compressive strength. As reported elsewhere, a decrease of the textural properties is also expected with increasing temperatures [19]–[21]. Therefore, a compromise between appropriate crushing strength and considerable textural properties is sought.

First, a study of the thermal stability of the SBA-15 powder was done. Thermal treatments between 550 °C (the typical temperature for thermal degradation of P123) and 1100 °C were conducted, and the textural and structural properties were probed using low-angle PXRD and N_2 physisorption. Following thermal treatment up to 950 °C, both the micro- and the mesoporous properties decreased with the temperature as observed on Figure 7. At 800 °C, the specific surface area was 20 % lower than at 550 °C (609 m²/g instead of 759 m²/g), and it was 56 % lower at 950 °C (334 m²/g). Figure S7 further shows the correlation between the thermal treatment and the final BET surface area and pore volume, with a rapid decline starting from 800 °C.

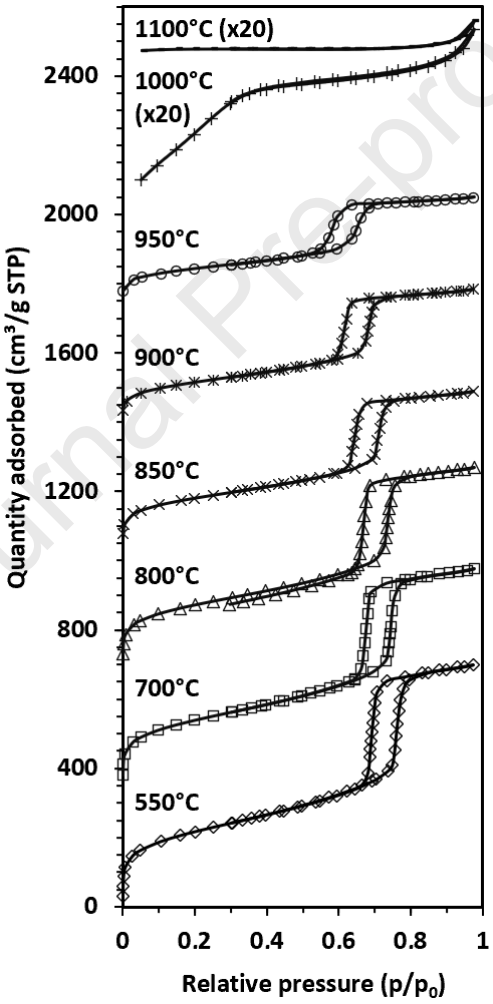

Figure 7: Nitrogen physisorption isotherms of SBA-15 powders treated at different temperatures. For the sake of clarity, isotherms are shifted vertically by 350 x n cm^3 STP/g, respectively (n = 0 to 6), except (g) which is shifted vertically by 1830 cm^3 STP/g and (b) surface areas and pores volumes of the same SBA-15 powders at different temperature.

Low-angle PXRD patterns (Figure S8) show a clear shift of peaks toward higher angles with increased temperatures. More specifically, the unit cell parameter (a_0) was reduced from 11.5 nm to 9.5 nm by

increasing the temperature, while the three peaks indexed to (100), (110) and (200) planes and corresponding to the P6mm arrangement remain visible up to 950 °C. This shrinkage of the SBA-15 structure is also apparent on the N_2 physisorption isotherm hystereses, which are shifted toward lower partial pressures (Figure 7). SEM images of the thermally-treated SBA-15 powders, provided in Figure S9, also show that as the temperature increases from 550 °C to 950 °C, the dimensions of the SBA-15 grains shrunk down by 30 %. All data are summarized in Table S3. Importantly, the hexagonal arrangement of the mesopores remains preserved up to 950 °C, as characterized by the parallel branches of the hystereses. Starting from 1000 °C, the SBA-15 structure completely collapses and most textural properties are lost. Therefore, for the monoliths a maximal temperature of 950 °C should be considered.

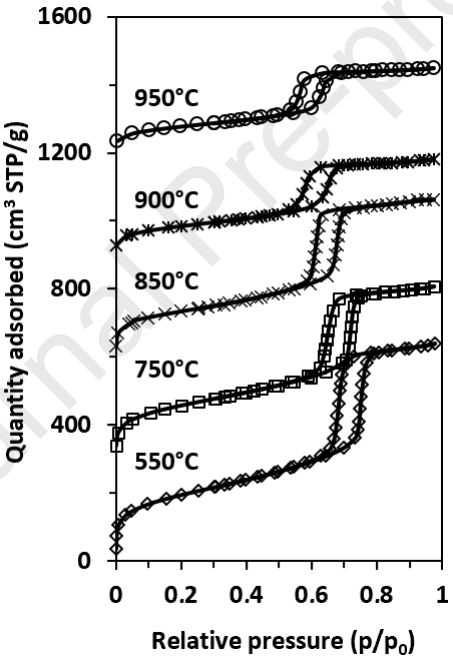

Figure 8: Nitrogen physisorption isotherms of SBA-15 monoliths prepared following the dispersion method and treated at different temperatures. For the sake of clarity, isotherms are shifted vertically by 300 x n cm^3 STP/g, respectively (n = 0 to 4).

Concerning monoliths, regardless of the method used to prepare hierarchical porous monoliths, similar modifications of the textural properties with temperature are observed. As in the case of the SBA-15 powder, the textural properties are significantly impacted by the treatment temperature, and starting from 900 °C the hysteresis shape is notably different, thus implying that the mesoporous ordering is modified (Figure 8 and Figure S10). From 420 °C to 900 °C, the specific surface area is halved (Table

2). The core and the outer surface of a monolith thermally treated at 950 °C were sampled. The comparable BET surface areas obtained ($S_{BET(core)}$ = 336 m²/g, $S_{BET(surface)}$ = 337 m²/g, see Figure S11) proves that the textural properties are homogeneous at the macroscale. Of note, the monoliths prepared by the dispersion method almost systematically present slightly higher BET surface areas, which could be due to the thicker macropore walls and hence a delaying effect of the thermal treatment on the SBA-15 grains located within the walls. The temperature also directly affects the monoliths diameter, which decrease from about 15.8 mm (550 °C) to 13.0 mm (950 °C) and further to 9.5 mm (1100 °C), while the objects macrostructural integrity remains even after treatment above 1100 °C (

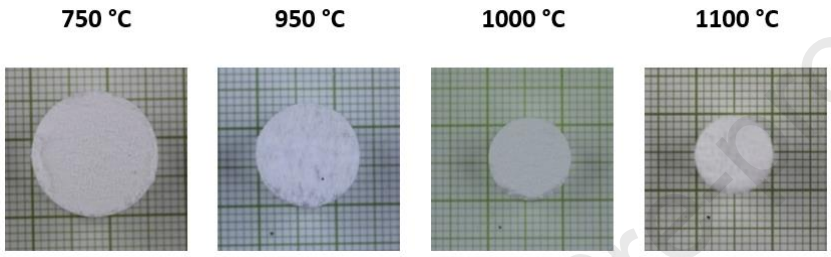

Figure 9).

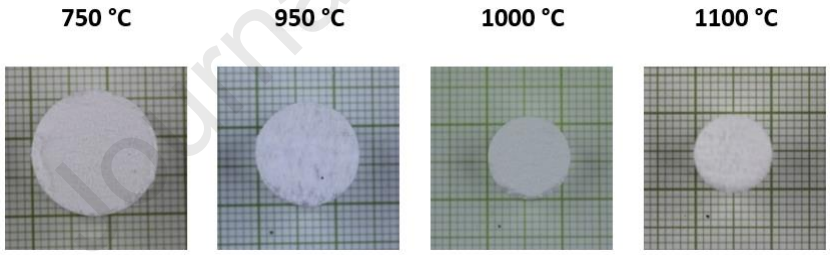

Figure 9: Photographs showing the temperature-related shrinkage of the monoliths obtained following the infiltration method.

Notably, as indicated in Table 2 a stronger influence of the temperature over the monoliths prepared following the dispersion method is observed. As no vacuum pump is used for this method, SBA-15 grains are likely to be in a looser arrangement compared to the infiltration method. And while SBA-15 grains are less compacted in the green monoliths, more voids are going to disappear during sintering, which will result in a greater shrinkage. This is confirmed by mercury intrusion porosimetry, as seen on Figure 10 and Figure S12. Independently of the method, the macropore volume decreases as the treatment temperature rises. This loss of macropore volume seems again more important for monoliths

prepared following the dispersion method, as their macropore volume decreases from 4.96 mL/g (420 °C) to 2.47 mL/g (1000 °C), whereas it decreases from 3.97 mL/g (420 °C) to 2.25 mL/g (1000 °C) for monoliths prepared by the infiltration method. A shrinkage of the interconnection windows is also observed, from 70 μm (420 °C) to 58 μm (1000 °C) and from 50 μm (420 °C) to 46 μm (1000 °C), respectively for monoliths prepared following the infiltration and the dispersion methods.

*Table 2: Comparison of the physical properties (diameter, crushing strength (**σ**), and specific surface area (S_{BET})) of the hierarchical porous monoliths prepared using a slurry of 10 wt.% SBA-15 following the infiltration and the dispersion methods.*

Treatment temperature (°C)	**Infiltration method**			**Dispersion method**		
	$D_{monolith}$ (mm)	**σ (kPa)**	**S_{BET} (m^2/g)**	**$D_{monolith}$ (mm)**	**σ (kPa)**	**S_{BET} (m^2/g)**
550	15.8	13	670	15.6	17	684
750	15.3	21	518	15.3	18	601
850	14.5	24	442	14.7	33	451
900	13.4	25	312	12.8	78	330
950	13.0	32	290	12.4	86	274
1000	12.0	64	< 50	-	-	-
1100	9.5	914	< 50	-	-	-

Meanwhile, as indicated in Table 2 and expected due to the densification of the monoliths, the crushing strength is clearly increased. Notably, the crushing strength of monoliths prepared following the dispersion method goes from 17 kPa (420 °C) to 78 kPa (900 °C). To better pinpoint the best compromise, Figure 11 shows the influence of the thermal treatment over both the crushing strength and the specific surface area.

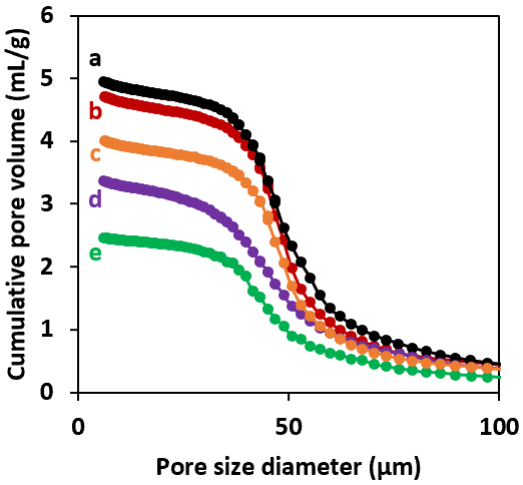

Figure 10: Mercury intrusion porosimetry of SBA-15 monoliths prepared following the dispersion method and treated at: (a) 550 °C, (b) 850 °C, (c) 900 °C, (d) 950 °C and (e) 1000 °C.

A temperature between 850 °C and 900 °C seems to be the most appropriate as relatively high specific surface areas are maintained while the crushing strength is clearly improved. Especially, following the dispersion method, monoliths treated at 850 °C present the same crushing strength than monoliths treated at 950 °C and prepared following the infiltration method (33 kPa and 32 kPa) while displaying higher specific surface area (451 m^2/g opposed to 290 m^2/g). By taking the examples of 850 and 900 °C as treatment temperatures, specific surface areas are similar for the infiltration and dispersion methods (442 and 312 m^2/g compared to 451 and 330 m^2/g, respectively). So the crushing strength differences cannot be explained by textural properties at the micro- and meso-scales. Of note, the macroporous volumes are quite different between the two methods used: 3.7 mL/g at 850 °C and 3.3 mL/g at 900 °C for infiltration while 4.8 mL/g at 850 °C and 4.0 mL/g at 900 °C for dispersion. The higher macroporous volumes obtained for the dispersion method should clearly be deleterious to mechanical properties, which is not the case. This is further illustrated by compressive mechanical tests conducted on dense monoliths, prepared without PMMA addition and presented on Figure S13. From 550 °C to 950 °C, the monoliths exhibit a crushing strength that is two orders of magnitude higher than the hierarchical monoliths (see Table S4), thus underlining the critical impact of the macroporous network over the mechanical resistance. This indicates that other features at least counterbalance the effect of macroporosity: the thicker macropore walls as underlined by SEM (Figure 4) and the smaller

interconnection diameters as shown by mercury intrusion porosimetry (Figure 10 and Figure S12) might compensate for the larger macropore volume.

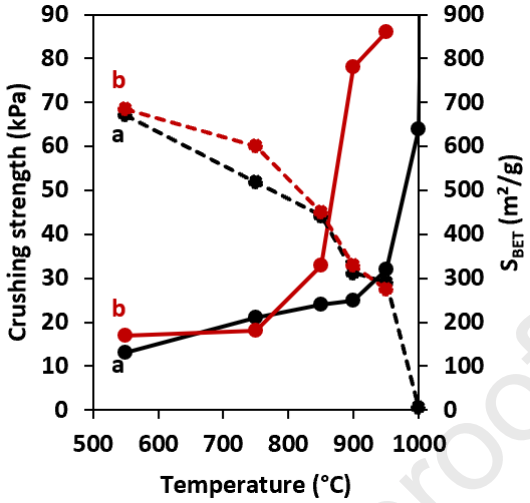

Figure 11: Crushing strength (full lines) and relating specific surface area (S_{BET}, dashed lines) according to the treatment temperature for monoliths prepared following (a, black) the infiltration method and (b, red) the dispersion method.

Of note, two other thermal treatments were also tried. One kept the same heating rate to reach the target temperature but with no plateau. The second thermal treatment involved 10 times higher heating rate (15 °C/min on average). However, as observed in Figure S14 no significant improvement was obtained. Indeed, when the results are expressed as a relationship between the obtained specific surface area over the crushing strength, a somehow linear relationship is observed.

4. Conclusions

Hierarchical porous monoliths were successfully prepared starting from PMMA beads and a SBA-15 slurry of optimized dynamic viscosity, following two methods: a classical dispersion-sedimentation method as well as an uncommon pathway based on the infiltration of a polymeric scaffold allowing optimizing the macropore interconnections. The resulting monoliths are highly porous (92 %) and the initial properties of the SBA-15 powder are preserved (-8% surface area), while displaying well-replicated macropores and adjustable ordering and interconnecting windows. As their mechanical resistance is rather low (around 15 kPa), thermal reinforcement was evaluated and an optimal temperature of 900 °C is proposed (up to 78 kPa for 330 m^2/g). These foam-like materials could be ideal

for applications under continuous flow, including the catalytic conversion of bulky molecules following a subsequent step of metal deposition.

Journal Pre-proof

Acknowledgments

The CNRS, the Chevreul Institute (FR 2638), the Ministère de l'Enseignement Supérieur et de la Recherche, the Région Hauts-de-France and the FEDER are acknowledged for supporting this work. Sébastien Royer acknowledges the Région Hauts-de-France for financial support through the UPCAT project. Ridvan Yildiz acknowledges the University of Lille and the Polytechnic University Hauts-de-France for the financial support for the PhD program.

References

[1] M. Hartmann and W. Schwieger, « Hierarchically-structured porous materials: from basic understanding to applications », *Chem. Soc. Rev.*, vol. 45, nº 12, p. 3311‑3312, 2016, doi: 10.1039/C6CS90043G.

[2] A. Feinle, M. S. Elsaesser and N. Hüsing, « Hierarchical Organization in Monolithic Sol–Gel Materials », in *Handbook of Sol-Gel Science and Technology*, L. Klein, M. Aparicio, et A. Jitianu, Éd. Cham: Springer International Publishing, 2016, p. 1‑49. doi: 10.1007/978-3-319-19454-7_127-1.

[3] J.-P. Dacquin, C. Ciotonea and S. Royer, « Synthesis Strategies and Emerging Catalytic Applications of Siliceous Materials with Hierarchically Ordered Porosity », in *Submicron Porous Materials*, P. Bettotti, Éd. Cham: Springer International Publishing, 2017, p. 189‑215. doi: 10.1007/978-3-319-53035-2_7.

[4] D. Zhao, « Triblock Copolymer Syntheses of Mesoporous Silica with Periodic 50 to 300 Angstrom Pores », *Science*, vol. 279, nº 5350, p. 548‑552, janv. 1998, doi: 10.1126/science.279.5350.548.

[5] A. Galarneau, H. Cambon, F. Di Renzo, R. Ryoo, M. Choi and F. Fajula, « Microporosity and connections between pores in SBA-15 mesostructured silicas as a function of the temperature of synthesis », *New J. Chem.*, vol. 27, nº 1, p. 73‑79, 2003, doi: 10.1039/b207378c.

[6] C. Ciotonea, I. Mazilu, B. Dragoi, C. Catrinescu, E. Dumitriu, A. Ungureanu, H. Alamdari, S. Petit and S. Royer, « Confining for Stability : Heterogeneous Catalysis with Transition Metal (Oxide) Nanoparticles Confined in the Secondary Pore Network of Mesoporous Scaffolds », *ChemNanoMat*, vol. 3, p 233-237, 2017, doi: 10.1002/cnma.201700014.

[7] C. Ciotonea, B. Dragoi, A. Ungureanu, C. Catrinescu, S. Petit, H. Alamdari, E. Marceau, E. Dumitriu and S. Royer, « Improved dispersion of transition metals in mesoporous materials through a polymer-assisted melt infiltration method: toward the genesis of micropore-confined highly dispersed metallic particles », *Catal. Sci. Technol.*, vol. 7, p 5448-5456, 2017, doi: 10.1039/C7CY00963A.

[8] J. Dhainaut, J.-P. Dacquin, A. F. Lee and K. Wilson, « Hierarchical macroporous–mesoporous SBA-15 sulfonic acidcatalysts for biodiesel synthesis », *Green Chem*, vol. 12, nº 2, p. 296‑303, 2010, doi: 10.1039/B919341C.

[9] J. Dhainaut, G. Piana, S. Deville, C. Guizard and M. Klotz, « Freezing-induced ordering of block copolymer micelles », *Chem Commun*, vol. 50, nº 83, p. 12572‑12574, 2014, doi: 10.1039/C4CC05556J.

[10] F. Putz, S. Scherer, M. Ober, R. Morak, O. Paris and N. Hüsing, « 3D Printing of Hierarchical Porous Silica and α-Quartz », *Adv. Mater. Technol.*, vol. 3, nº 7, p. 1800060, 2018, doi: 10.1002/admt.201800060.

[11] T. Amatani, K. Nakanishi, K. Hirao and T. Kodaira, « Monolithic Periodic Mesoporous Silica with Well-Defined Macropores », *Chem. Mater.*, vol. 17, nº 8, p. 2114‑2119, 2005, doi: 10.1021/cm048091c.

[12] F. Carn, A. Colin, M.-F. Achard, H. Deleuze, E. Sellier, M. Birot and R. Backov, « Inorganic monoliths hierarchically textured via concentrated direct emulsion and micellar templates », *J. Mater. Chem.*, vol. 14, nº 9, p. 1370, 2004, doi: 10.1039/b400984c.
[13] M. Descamps, T. Duhoo, F. Monchau, J. Lu, P. Hardouin, J. C. Hornez and A. Leriche, « Manufacture of macroporous β-tricalcium phosphate bioceramics », *J. Eur. Ceram. Soc.*, vol. 28, nº 1, p. 149‑157, 2008, doi: 10.1016/j.jeurceramsoc.2007.05.025.
[14] M. Descamps, O. Richart, P. Hardouin, J. C. Hornez and A. Leriche, « Synthesis of macroporous β-tricalcium phosphate with controlled porous architectural », *Ceram. Int.*, vol. 34, nº 5, p. 1131‑1137, 2008, doi: 10.1016/j.ceramint.2007.01.004.
[15] A. Sachse, A. Galarneau, F. Fajula, F. Di Renzo, P. Creux, B. Coq, « Functional silica monoliths with hierarchical uniform porosity as continuous flow catalytic reactors », *Micro. Meso. Mater.*, vol. 140, nº 1-3, p. 58-68, 2011, doi: 10.1016/j.micromeso.2010.10.044.
[16] H. Pérez, P. Navarro and M. Montes, « Deposition of SBA-15 layers on Fecralloy monoliths by washcoating », *Chem. Eng. J.*, vol. 158, nº 2, p. 325‑332, 2010, doi: 10.1016/j.cej.2010.01.032.
[17] L. J. Gibson and M. F. Ashby, *Cellular Solids: Structure and Properties*, 2e éd. Cambridge University Press, 1997. doi: 10.1017/CBO9781139878326.
[18] A. R. Studart, U. T. Gonzenbach, E. Tervoort and L. J. Gauckler, « Processing Routes to Macroporous Ceramics: A Review », *J. Am. Ceram. Soc.*, vol. 89, nº 6, p. 1771‑1789, 2006, doi: 10.1111/j.1551-2916.2006.01044.x.
[19] R. Ryoo and C. H. Ko, « Block-Copolymer-Templated Ordered Mesoporous Silica: Array of Uniform Mesopores or Mesopore-Micropore Network? », *J. Phys. Chem. B*, vol. 104, nº 48, p. 11465‑11471, 2000, doi: 10.1021/jp002597a.
[20] Y. Usami, T. Hongo and A. Yamazaki, « Thermal stability and behavior of platelet-shaped SBA-15 containing Zr », *J. Porous Mater.*, vol. 19, nº 5, p. 897‑902, 2012, doi: 10.1007/s10934-011-9547-9.
[21] J. B. Lowe and R. T. Baker, « Deformation of Ordered Mesoporous Silica Structures on Exposure to High Temperatures », *J. Nanomater.*, vol. 2014, p. 1‑13, 2014, doi: 10.1155/2014/754076.

Journal Pre-proof

Journal Pre-proof

Highlights

- Preformed polymeric scaffolds infiltrated by SBA-15 slurries
- Self-supported materials with calibrated hierarchical porosity obtained
- Thermal treatment increases the mechanical resistance at the expense of both mesoporosity and macroporosity

Journal Pre-proof

Journal Pre-proof

Declaration of interests

☒ The authors declare that they have no known competing financial interests or personal relationships that could have appeared to influence the work reported in this paper.

☐ The authors declare the following financial interests/personal relationships which may be considered as potential competing interests:

Journal Pre-proof